

Microstructural evolution in MgO_p/AlN composites

Y.W. Li^a, S.L. Jin^{a,*}, Y.B. Li^a, L. Zhao^a, Z.Y. Li^b

^a State Key Laboratory Breeding Base of Refractories and Ceramics, Wuhan University of Science and Technology, Wuhan, 430081, China

^b Shanghai Baosteel Institute, Shanghai, 201900, China

Received 17 July 2008; received in revised form 1 October 2008; accepted 27 December 2008

Available online 22 January 2009

Abstract

MgO_p/AlN composite has been fabricated by directed melt nitridation of pure Al block covered with a powder mixture of 0.5–1 mm magnesia particles and 0.075–0.15 mm chemically pure magnesium powder in flowing N_2 in the range of 900–1200 °C. The extent of Al nitridation and the depth of Al penetration into the MgO particles increases with temperature. The phase composition in the matrix from metal rich to ceramic rich can be adjusted by controlling processing temperature. A multilayer microstructure of $\text{MgO}/\text{MgAl}_2\text{O}_4/\text{AlN}$ surrounds the MgO particles due to the interface reaction. The thickness of each layer in this structure varies with processing parameters such as the temperature and local Mg concentration, depending on the influence of these processing parameters on the interface reaction of MgAl_2O_4 formation and Al nitridation. © 2009 Elsevier Ltd and Techna Group S.r.l. All rights reserved.

Keywords: B. Interface; D. Nitride; D. MgO; E. Refractories

1. Introduction

Magnesia–graphite slide gates have often been used for casting higher calcium-alloy-treated steels [1]. However, they are unsuitable for multiple heat operations, because magnesia–graphite slide gates have poor spalling resistance due to the large thermal expansion coefficient of magnesia ($10.8\text{--}15 \times 10^{-6} \text{ K}^{-1}$, 20–1000 °C). Multiple-heat-operation slide gates demand improved spalling resistance of the materials system. Aluminum nitride has a high thermal conductivity (140–170 W/m K), lower thermal expansion coefficient ($5.4 \times 10^{-6} \text{ K}^{-1}$, 20–1000 °C) and better corrosion resistance to steel melt and slag, and is a promising ceramic material in iron and steel industry [2]. Reinforced with AlN, MgO composite material is regarded as a new generation of refractory with excellent thermal shock resistance and corrosion resistance to replace magnesia–graphite composites in many applications.

Directed melt nitridation originated from the directed melt oxidation process initiated by Newkirk et al. [3]. This method offers the ability to adjust the composite properties by selecting different processing parameters such as matrix compositions and processing temperatures. It is also a low cost process,

especially with the elimination of possible damage caused by densification shrinkage. It facilitates manufacture of very large ceramic bodies with near-net-shape and has thus attracted much interest. Many composites have been fabricated by infiltration and nitridation of Al, Al–Mg or Al–Mg–Si alloys into Al_2O_3 or SiC reinforcement materials [4–7]. MgO composite reinforced with AlN also have been reported by Lanxide Company with DIMOXTM technology [8,9]. However, there have been no detailed studies of the microstructure of MgO/AlN composites.

In this paper, MgO_p/AlN composites were prepared through directed melt nitridation of pure Al blocks using Mg powder as an external dopant, in order to avoid the second smelting of Al and Mg. The microstructure characteristics and interface reactions of MgO_p/AlN composite were investigated to understand the influence of processing temperature on the composite growth.

2. Experimental procedures

Pure Al blocks (>99 wt.%) were contained in a small graphite crucible with corundum powder as barrier material, and 10 wt.% 0.075–0.15 mm chemically pure Mg powder (>99 wt.%) was simply mixed with 0.5–1 mm fused magnesia (>98 wt.% MgO , abbreviated as MgO_p) by mechanical apparatus, then loosely packed on the surface of Al blocks, as shown in Fig. 1. The reactor tube was evacuated (<100 Pa) and then refilled with high

* Corresponding author. Tel.: +86 27 68862188; fax: +86 27 68862018.

E-mail address: kingsleref@hotmail.com (S.L. Jin).

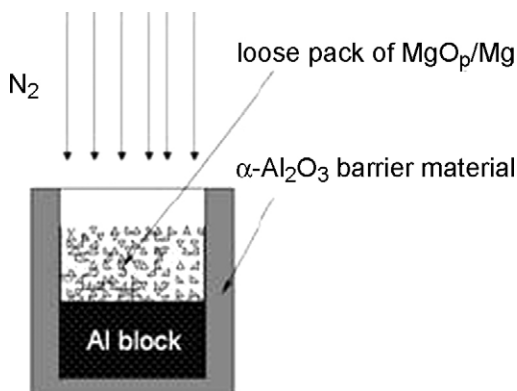


Fig. 1. Configuration of the block/preform assembly.

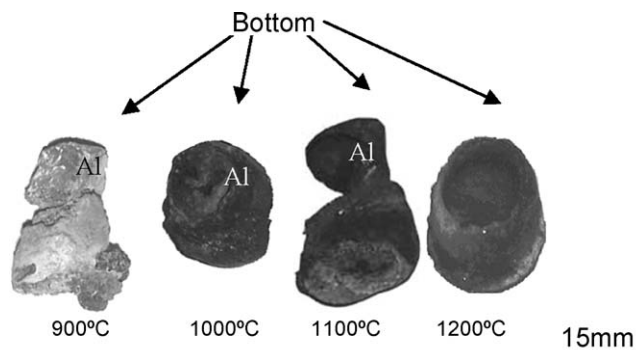


Fig. 2. Appearance of samples prepared at different temperatures.

purity N_2 (99.999%) three times at 373 K to purify the atmosphere. N_2 was flowed at a rate of 20 ml/min to simulate the stable atmosphere during the experiment. To avoid the entry of air into the system, the outgoing gas was bubbled through a column of water before being vented into the atmosphere. The furnace was heated at a rate of $10^\circ\text{C}/\text{min}$. When the temperature reached the reaction temperatures in the range of 900 – 1200°C , the whole assembly was quickly lowered to the hot zone and soaked for 10 h. The furnace was cooled naturally to room temperature with N_2 flowing until 660°C .

The weight of whole sample assembly before and after nitridation was measured in order to calculate the nitridation rate. The nitridation rate α was calculated according to the reaction (1).



$$\alpha = \frac{m_{\text{rp}} - m_{\text{Al}}}{m_{\text{Al}}} \quad (2)$$

where m is the weight of the original Al block and the reaction product (rp). At high temperature, magnesium existed as a vapor and was assumed to evaporate from the crucible. It might deposit on the surface of the furnace tube in the form of either MgO or Mg_3N_2 depending on the oxygen content in the flowing N_2 . Therefore, the influence of magnesium on weight change can be neglected [10]. As a result, the weight gain reflects the extent of Al melt nitridation.

After experiments, the as-received samples were sectioned longitudinally and polished for microstructure observation using optical microscopy (OM, Zeiss Axoskop 40Apol) and electron probe microanalysis (EPMA, JXA8800R). The matrix hardness of as-received samples was measured with a hardness tester (HM-114, Akashi) using a test load of 50 g. Also, as-received samples were investigated by X-ray diffraction (XRD, Philips MPD Pro) to identify the phase composition.

3. Results and discussion

3.1. Phase and microstructure characteristics

Fig. 2 shows the appearance of samples obtained after various heat treatments. After 10 h at 900°C , the sample is grey

and obviously the magnesite preform has not been completely penetrated. A significant volume of pure Al was found at the bottom of the composites. After 10 h at 1000 and 1100°C , the sample turns dark with an irregular shape and less remnant Al. After 1200°C , the sample retains its cylindrical with no remnant Al. The weight gains of as-received samples increase from 26.2% to 36.5% as temperature increases from 900 to 1200°C (Fig. 3). This indicates that the higher processing temperature benefits both the nitridation and penetration of Al into magnesite particles.

The longitudinally polished sections of as-received samples were examined by XRD (Fig. 4). For the samples prepared at 900°C , AlN phase was detected except periclase, and Al in the product. Above 1000°C , significant levels of magnesium aluminum spinel appeared in the product but then decreased at higher temperatures, and Al was consumed as temperature increased.

Optical microscopy (Fig. 5) revealed in the sample prepared at 900°C that white metal phase was surrounded and separated by grey ceramic phase in the matrix between grey magnesite particles. After 10 h at 1000°C , the mixture of metal and ceramic phases was found in the matrix between grey magnesite particles and the matrix closely adhered to the MgO. After 1100°C , a little of the metal was still present and the matrix structure was relatively loose. Over 1200°C , the white metal

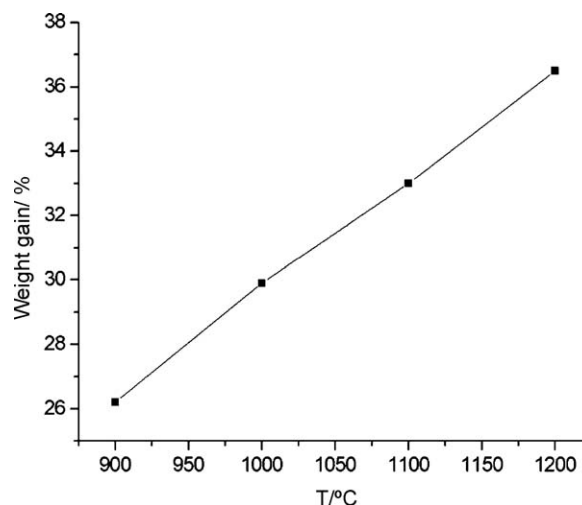


Fig. 3. Weight gain as a function of processing temperature.

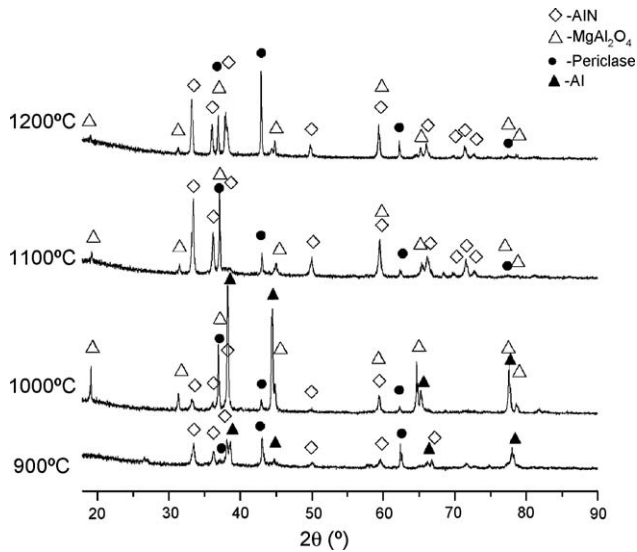


Fig. 4. XRD patterns of samples prepared at 900–1200 °C.

was consumed and the space among the magnesia particles was almost completely filled with ceramic phase.

The matrix hardness (Table 1) in samples with a metal-rich matrix, increased with temperature whereas it remained constant samples with a ceramic-rich matrix. In the samples obtained at temperatures over 1100 °C, it was hard to distinguish metal-rich and ceramic-rich portions, which caused fluctuation in the measured hardness data. However, in the sample produced at 1200 °C, the maximum microhardness was 11.2 GPa, approaching that of pure AlN (12 GPa).

The microstructure of samples was also studied by EPMA. Four different layers can be clearly distinguished in the sample

Table 1

Microhardness of matrix in the samples prepared at different temperatures.

Temperature (°C)	Matrix hardness (GPa)	
	Metal-rich portion	Ceramic-rich portion
900	1.52	5.08
1000	2.35	5.08
1100	–	3.81–4.56
1200	–	6.03–11.2

prepared at 1000 °C (Fig. 6). The first was a small MgO layer (Point 1), which was surrounded by a ~50 μm thick MgAl₂O₄ layer (Point 2). This reveals that most of the original MgO particle has been eroded by Al since 0.5–1 mm MgO particles were used in this experiment. While the third, close to MgAl₂O₄ layer, was a ~20 μm thick AlN layer (Point 3). The fourth layer which is immediately next to the AlN layer was matrix growth, consisting of AlN and Al (Point 4). It is interesting that Mg was always found in both the AlN layer and the matrix. Although Mg₃N₂ and AlN can be a solid solution [11], it is still hard to say whether it had an AlN–Mg₃N₂ solid solution or not, because Mg also can be detected by EPMA if Mg was trapped at intact Al. In addition, a different three-layer microstructure was found in different locations of the same product, where MgO particle was directly adjacent to AlN layer and only a small amount of Al was left (Fig. 7). For samples prepared at 1100 °C, the different three-layer microstructure of MgO/MgAl₂O₄/AlN can often be found and the matrix completely consisted of AlN, as seen in Fig. 8. However, the thickness of MgAl₂O₄ layer was thin approaching ~10 μm. This reveals the thickness of MgAl₂O₄ layer was relevant to the processing parameters and the reaction extent at

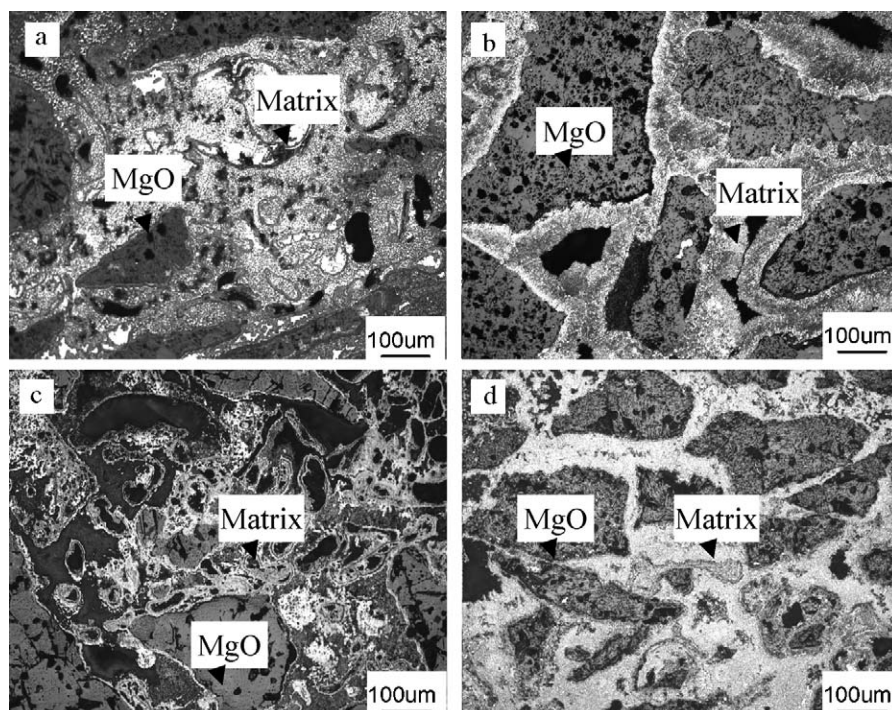


Fig. 5. Optical microstructures of samples prepared at (a) 900 °C, (b) 1000 °C, (c) 1100 °C, and (d) 1200 °C.

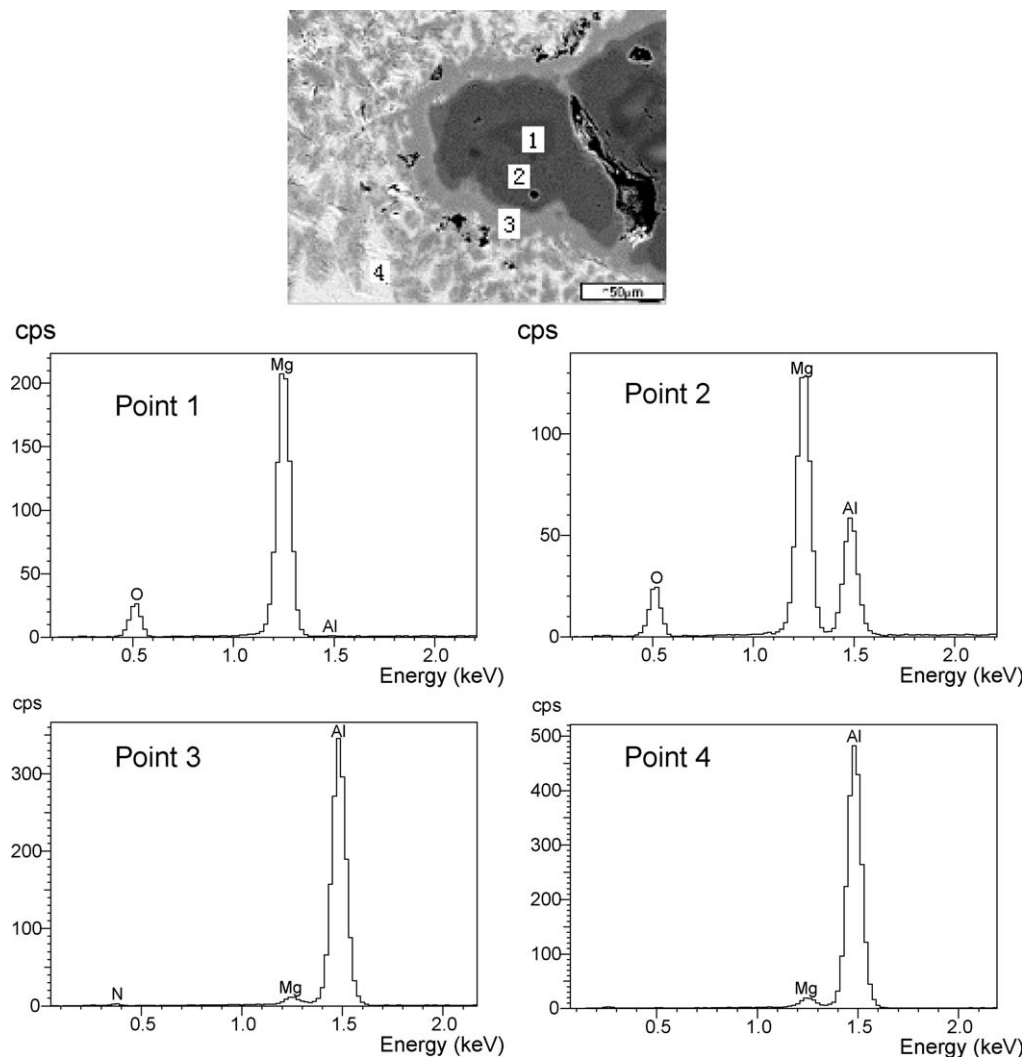


Fig. 6. Four-layer microstructure of the sample prepared at 1000 °C.

different regions was heterogeneous and affected by the local conditions.

3.2. Discussion

Nitridation and infiltration of Al were promoted by processing temperature as revealed by the weight gain and shape of the product. According to the results of XRD and SEM, a lot of Al was left not only in the composite but also in parent alloy at lower processing temperatures indicating that capillary transport mainly governed matrix growth over this range of temperatures. Besides, nitridation was controlled by the diffusion of nitrogen through the surface AlN layer at low temperatures [10]. Therefore, the more rapidly the liquid/vapor interface moved into the preform, the lower the content of the nitrogen that was picked up. After 1100 and 1200 °C, little Al was found inside the composite but remnant Al alloy still was found after 1100 °C. It appears that Al nitridation occurred prior to Al infiltration at higher temperature. Thus, the influence of processing temperature on the nitridation reaction was expected to be greater than on factors such as viscosity and

surface tension at higher temperature, which dictated the capillarity-induced flow of metal according to the findings of Martins et al. [12], who developed an infiltration rate parameter, φ , as expressed as

$$\varphi = \frac{(r\gamma_{LV} \cos \theta)}{2\mu} \quad (3)$$

where $(r\gamma_{LV} \cos \theta)$ is the surface tension force term and μ is the viscosity of the melt. According to this equation, enhancing processing temperature accelerates the infiltration by decreasing the viscosity and surface tension, since the viscosity of Al alloy decreased faster than surface tension force [13]. However, large conversion of Al into AlN has an adverse influence on the infiltration by reducing the capillary radius as also determined by Jin et al. [14]. Therefore, infiltration of Al and nitridation of Al were competitive and interactive processes. Finally the nitridation dominated the growth of the MgO_p/AlN composite. This is consistent with Nagendra et al., who found that lower processing temperature promoted infiltration of Al whereas higher one accelerated nitridation of Al, when Al–Mg alloys

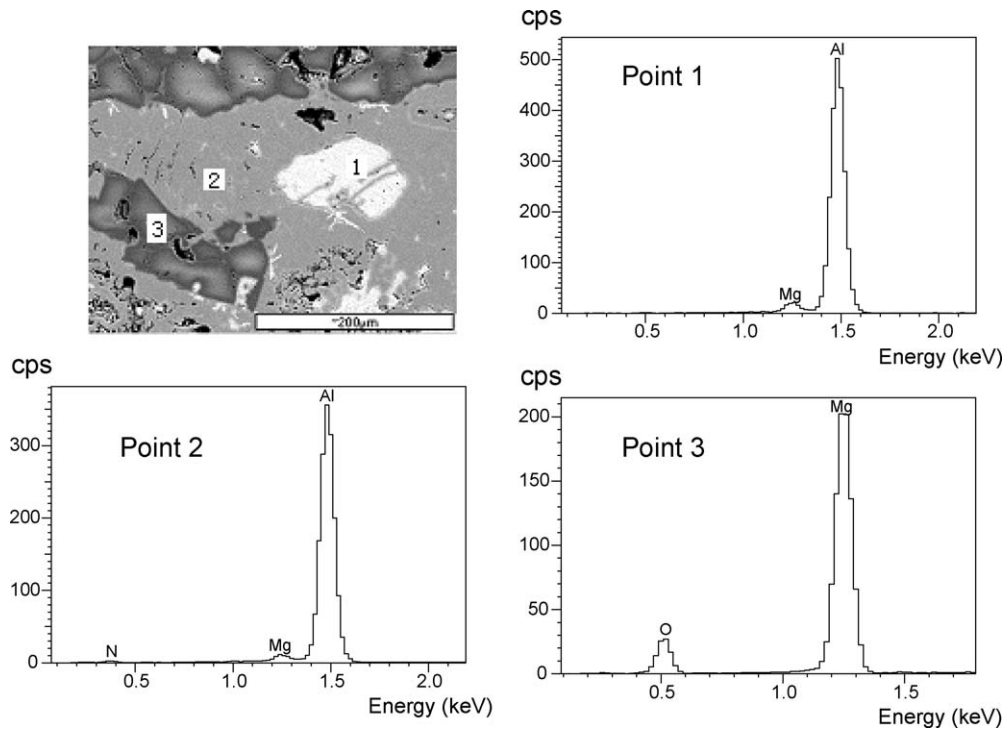


Fig. 7. Three-layer microstructure of the sample prepared at 1000 °C.

were infiltrated into an Al_2O_3 preform over N_2 or $\text{N}_2\text{--H}_2$ in the temperature range 900–1200 °C [15].

The corrosion of MgO by Al was obvious during the experiment. However, the depth of penetration and corrosion did not become greater with increase of processing temperature as was expected. The different content of Mg at the local region

plays an important role in the microstructural evolution of these MgO_p/Al composites. For the nitridation process of Al with external dopant Mg, the major Mg source was the Mg powder dopant, which was easily vaporized and lost at high temperature even when Al–Si–Mg alloy was used during pressureless infiltration process, where the amount of Mg lost was about

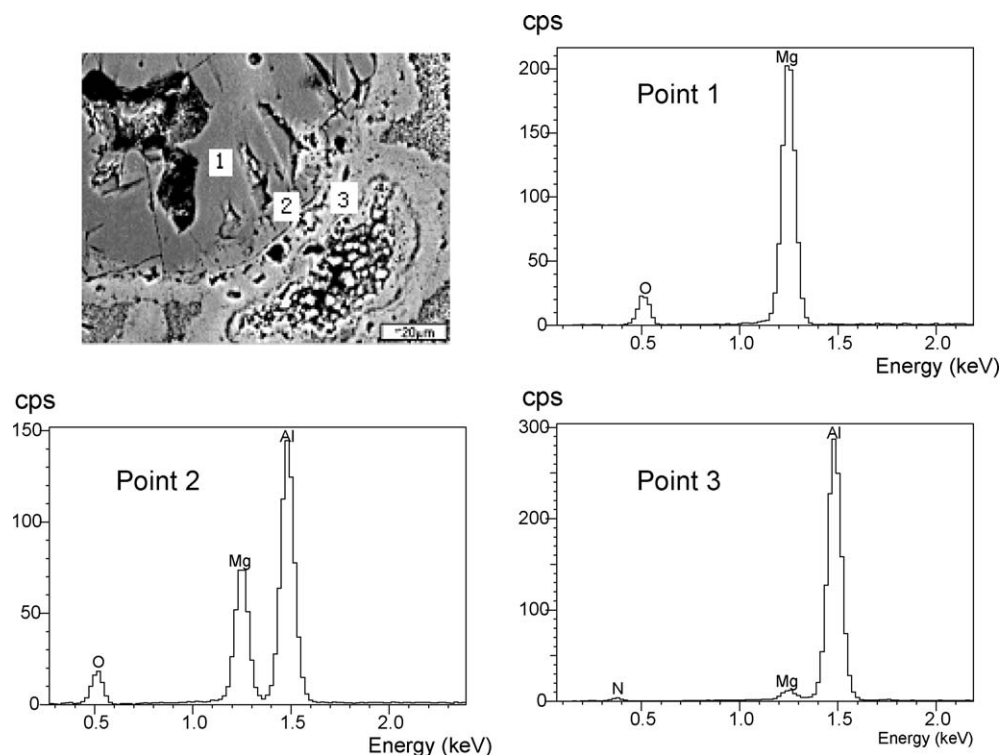
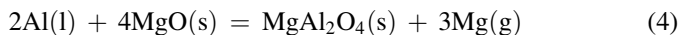


Fig. 8. Three-layer microstructure of the sample prepared at 1100 °C.

60 wt.% at 995–1020 °C and almost all the Mg was lost at 1215 °C [16], no mention that Mg was mixed simply with MgO particles by mechanical apparatus at our experiment. Another source of Mg was that derived from the interface reaction between Al and MgO to form spinel according to reaction (4):



This reaction was thermodynamically favoured at lower temperatures since the least amount of Mg in equilibrium with MgAl_2O_4 increased with temperature [17] and was possible at all processing temperatures since the original Mg content was 10 wt.%. Considering the kinetics of the process, the formation of the spinel interface reaction started with the counter-diffusion of Al^{3+} and Mg^{2+} in MgO, after which the nucleation of MgAl_2O_4 took place. Whitney and Stubican [18] reported the self-diffusion coefficient of Al^{3+} in MgO at 1600 °C to be $8.4 \times 10^{-15} \text{ m}^2/\text{s}$ and Zhang et al. [19] found the volume of MgO with Al diffused in it increased with the temperature. Therefore, $\sim 2.24 \mu\text{m}$ thickness of MgO should form into MgAl_2O_4 after 10 h at 1600 °C and the thickness of MgAl_2O_4 should be much less at lower temperature. However, this is in contrast to our observations of the minimum thickness of the MgAl_2O_4 layer, which was about 10 μm and decreased as the processing temperature increased. This might be related to the different processing conditions adopted during the experiment; herein nitrogen atmosphere was specially used. The nitridation of Al and formation of MgAl_2O_4 happened synchronously and were competitive and interactional. Formation of MgAl_2O_4 took place and was further favoured at low temperatures through prolonged contact between MgO and Al [20]. Thus, a thicker MgAl_2O_4 layer was produced (Figs. 6 and 9a), which accompanied the release of Mg (g). Scholz and Griel reported that high magnesium content accelerated the volume of nitrided metal [10]. Therefore, the localized increase of Mg would benefit the nitridation of Al adjacent to MgO particles, and then a dense AlN layer formed easily. As the reactions progressed and the pores between MgO particles were gradually filled, some Mg was trapped in these pores due to the aggregation of MgO particles sealed with Al melt, and the nitridation of Al would be promoted due to the large amount of Mg present at the reaction frontier. Thus, the nitridation

reaction became a predominant reaction process for this area and Al was rapidly depleted by nitridation with no formation of an MgAl_2O_4 layer, as seen in Figs. 7 and 9b. Above 1100 °C, the influence of temperature on the nitridation was also expected to be greater than on the formation of MgAl_2O_4 and most Al was quickly exhausted by nitridation. Compared to the interface of MgO particles with Al at 1000 °C, the MgAl_2O_4 layer at 1100 and 1200 °C was much thinner and Al was almost completely transformed to AlN, as seen in Figs. 8 and 9c.

4. Conclusions

Pure Al block has been successfully penetrated into and nitrided on the mixture of 0.5–1 mm MgO particles with 10 wt.% Mg powder to fabricate MgO_p/AlN composite. The matrix composition in the composite changed from metal-rich to ceramic-rich as temperature increased from 900 to 1200 °C.

A multilayer microstructure was observed surrounding MgO particles in all samples and formed through reactions among Al, MgO and N_2 . Increasing the processing temperature enhanced the nitridation rate of Al and suppressed the interface between MgO particles with Al into MgAl_2O_4 . An inhomogeneous vapor distribution of Mg changed the microstructure of composites in local regions.

Acknowledgements

The authors are grateful for the financial support by National Natural Science Foundation of China, under Grant No. 50572076 and Ministry of Education of China under Grant No. 20040488001. They also thank Professor Xiang Z.D. for providing valuable suggestions during writing this paper and Engineer Wu X.J. for helping them to smelt Al block.

References

- [1] K. Akamine, S. Nitawaki, T. Kaneko, M. Harada, MgO–C sliding nozzle plate for casting calcium-alloy-treated steel, *Taikabutsu Overseas* 18 (1) (1998) 22–27.
- [2] A. Amadeh, S. Heshmati-Manesh, J.C. Labbe, A. Laimeche, P. Quintard, Wettability and corrosion of TiN, TiN–BN and TiN–AlN by liquid steel, *J. Eur. Ceram. Soc.* 21 (3) (2001) 277–282.
- [3] M.S. Newkirk, H.D. Leshner, D.R. White, C.R. Kennedy, A.W. Urquhart, T.D. Claar, Preparation of Lanxide™ ceramic matrix composites: matrix formation by the directed oxidation of molten metals, *Ceram. Eng. Sci. Proc.* 8 (7–8) (1987) 879–885.
- [4] S.L. Jin, Y.W. Li, Y.B. Li, L. Zhao, Z.Y. Li, Modified directed melt nitridation of pure aluminum block using magnesium as an external dopant, *J. Mater. Sci.* 42 (17) (2007) 7311–7313.
- [5] S. Swaminathan, R.B. Srinivasa, V. Jayaram, The influence of oxygen impurities on the formation of AlN–Al composites by infiltration of molten Al–Mg, *Acta Mater.* 50 (2002) 3093–3104.
- [6] B. Daniel, V.S.R. Murthy, Microstructure and mechanical properties of SiC reinforced AlN/Al composites, *ISIJ Int.* 37 (10) (1997) 992–999.
- [7] M.K. Aghajanian, J.P. Biel, R.G. Smith, AlN matrix composites fabricated via an infiltration and reaction approach, *J. Am. Ceram. Soc.* 77 (7) (1994) 1917–1920.
- [8] D.R. McLachlan, J.A. Kuszyk, *Advances in Refractories for the Metallurgical Industries*, Montreal, Quebec, Canada, 24–29, Aug, 1996, pp.329–337.
- [9] E. Ruh, Worldwide trends in refractories, *Ceram. Ind.* (1995) 31–38.

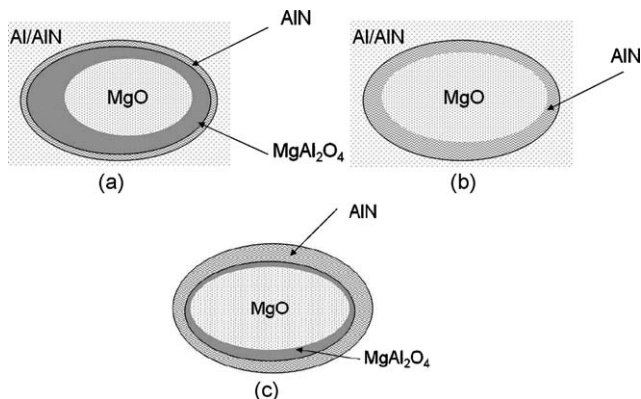


Fig. 9. Schematic diagram of growth mechanism of MgO_p/AlN (a and b at lower temperature, c at higher temperature).

- [10] H. Scholz, P. Greil, Nitridation reactions of molten Al–(Mg,Si) alloys, *J. Mater. Sci.* 26 (1991) 669–677.
- [11] R.P. Lesunova, E.I. Burmakin, Electrical conductivity of AlN–Mg₃N₂ solid solutions, *Inorg. Mater. (Russia)* 44 (7) (2005) 819–822.
- [12] G.P. Martins, D.L. Olsen, G.R. Edwards, Modeling of infiltration kinetics for liquid metal processing of composites, *Met. Trans.* 19B (1998) 95–101.
- [13] J.E. Hatch, *Aluminum: Properties and Physical Metallurgy*, American Society for Metals, Metals Park, Ohio, USA, 1988.
- [14] S.L. Jin, Y.W. Li, G.T. Liu, Y.B. Li, L. Zhao, Z.Y. Li, Magnesium vapor diffusion behavior over Al molten surface in directed metal nitridation process, *Rare Met. Mater. Eng. (China)* 37 (1) (2008) 58–61.
- [15] N. Nagendra, B.S. Rao, V. Jayaram, Microstructures and properties of Al₂O₃/Al–AlN composites by pressureless infiltration of Al-alloys, *Mater. Sci. Eng.* A269 (1999) 26–37.
- [16] T. Debroy, A. Bandopadhyay, R. Roy, Oxide matrix composite by directional oxidation of a commercial aluminum–magnesium alloy, *J. Am. Ceram. Soc.* 77 (5) (1994) 1296–1300.
- [17] M. Rodriguez-Reyes, M.I. Pech-Canul, E.E. Parras-Medecigo, A. Gorokhovskiy, Effect of Mg loss on the kinetics of pressureless infiltration in the processing of Al–Si–Mg/SiCp composites, *Mater. Lett.* 57 (2003) 2081–2089.
- [18] W.P. Whitney II, V.S. Stubican, Interdiffusion studies in the system MgO–MgAl₂O₄, *J. Am. Ceram. Soc.* 54 (7) (1971) 349–352.
- [19] P. Zhang, T. Debroy, S. Seetharaman, Interdiffusion in the MgO–Al₂O₃ spinel with or without some dopants, *Metall. Mater. Trans. A* 27A (8) (1996) 2105–2113.
- [20] O. Salas, V. Jayaram, K.C. Vlach, C.G. Levi, R. Mehrabian, Early stages of composite formation by oxidation of liquid aluminum alloys, *J. Am. Ceram. Soc.* 78 (3) (1995) 609–622.